

# Phosphatidylinositol 4,5-Bisphosphate Induces Actin Stress-fiber Formation and Inhibits Membrane Ruffling in CV1 Cells

Masaya Yamamoto,\* Donald H. Hilgemann,\* Siyi Feng,\* Haruhiko Bito,‡ Hisamitsu Ishihara,§ Yoshikazu Shibasaki,§ and Helen L. Yin\*

\*Department of Physiology, University of Texas Southwestern Medical Center, Dallas, Texas 75390; ‡Department of Pharmacology, Kyoto University Faculty of Medicine, Kyoto, TOREST-JST, Japan; and §Department of Metabolic Diseases, University of Tokyo, Tokyo, Japan

**Abstract.** Phosphatidylinositol 4,5 bisphosphate (PIP<sub>2</sub>) is widely implicated in cytoskeleton regulation, but the mechanisms by which PIP<sub>2</sub> effect cytoskeletal changes are not defined. We used recombinant adenovirus to infect CV1 cells with the mouse type I phosphatidylinositol phosphate 5-kinase  $\alpha$  (PIP5KI), and identified the players that modulate the cytoskeleton in response to PIP<sub>2</sub> signaling. PIP5KI overexpression increased PIP<sub>2</sub> and reduced phosphatidylinositol 4 phosphate (PI4P) levels. It promoted robust stress-fiber formation in CV1 cells and blocked PDGF-induced membrane ruffling and nucleated actin assembly. Y-27632, a Rho-dependent serine/threonine protein kinase (ROCK) inhibitor, blocked stress-fiber formation and inhibited PIP<sub>2</sub> and PI4P synthesis in cells. However, Y-27632 had no effect

on PIP<sub>2</sub> synthesis in lysates, although it inhibited PI4P synthesis. Thus, ROCK may regulate PIP<sub>2</sub> synthesis by controlling PI4P availability. PIP5KI overexpression decreased gelsolin, profilin, and capping protein binding to actin and increased that of ezrin. These changes can potentially account for the increased stress fiber and non-ruffling phenotype. Our results establish the physiological role of PIP<sub>2</sub> in cytoskeletal regulation, clarify the relation between Rho, ROCK, and PIP<sub>2</sub> in the activation of stress-fiber formation, and identify the key players that modulate the actin cytoskeleton in response to PIP<sub>2</sub>.

**Key words:** phosphatidylinositol 4,5 bisphosphate • Rho • Rho-dependent serine/threonine kinase • gelsolin • phosphatidylinositol phosphate 5-kinase

## Introduction

Phosphatidylinositol 4,5 bisphosphate (PIP<sub>2</sub>)<sup>1</sup> modulates many actin regulatory proteins in vitro (Yin and Stull, 1999), and manipulations of intracellular PIP<sub>2</sub> levels have profound effects on the actin cytoskeleton. Overexpression of a 5'-PIP<sub>2</sub> phosphatase to change PIP<sub>2</sub> level (Sakisaka et al., 1997), or a pleckstrin homology domain of PLC $\delta$  to sequester PIP<sub>2</sub> dissipates actin stress fibers and decreases the attachment of stress fibers to the plasma membrane (Raucher et al., 2000). Deletion of a 5'-PIP<sub>2</sub> phosphatase gene severely compromises synaptic vesicle recycling (Cremona et al., 1999). Overexpression of type I phosphatidyl-

inositol phosphate 5-kinase (PIP5KI), the enzyme that accounts for most of the synthesis of PIP<sub>2</sub> from phosphatidylinositol 4-phosphate (PI4P), induces dramatic actin rearrangements. Paradoxically, there is a wide range of actin phenotypes, depending on the type of cells used. These include comet-like actin tails (Rozelle et al., 2000), microvilli (Matsui et al., 1999), membrane ruffles (Honda et al., 1999), and abnormal pine needle-like structures (Shibasaki et al., 1997). It is difficult to explain why overexpression of the same enzyme has pleiotropic effects. One potential explanation is that the different cell backgrounds may favor a unique combinatorial involvement of subsets of potential players. For example, many small GTPases including Rho (Chong et al., 1994; Weernink et al., 2000), Rac (Tolias et al., 2000), Arf6 (Honda et al., 1999), and Arf1 (Jones et al., 2000) affect PIP5KI activity, and many actin regulatory proteins are regulated by PIP<sub>2</sub> in vitro. The large number of potential upstream regulators and downstream effectors of PIP5KI and the use of transient PIP5KI overexpression have confounded biochemical analysis. Thus there is still considerable disagreement as to which small GTPases are required, and the major players that

Address correspondence to Helen L. Yin, Ph.D., Dept. of Physiology, University of Texas Southwestern Medical Center, 5323 Harry Hines Blvd., Dallas, TX 75390. Tel.: 214-6487967. Fax: 214-6487891. E-mail: helen.yin@utsouthwestern.edu

<sup>1</sup>Abbreviations used in this paper: ADF, actin depolymerizing factor; BDM, 2,3-butanedione 2 monoxide; ERM, ezrin/radixin/moesin; HA, hemagglutinin; HSP, high-speed pellet; HSS, high-speed supernatant; LSP, low-speed pellet; PI4P, phosphatidylinositol 4 phosphate; PIP<sub>2</sub>, phosphatidylinositol 4,5 bisphosphate; PIP5KI, type I phosphatidylinositol phosphate 5-kinase  $\alpha$ ; PS, phosphatidylserine; ROCK, Rho-dependent serine/threonine kinase; TLC, thin layer chromatography.

generate a particular cytoskeletal phenotype after PIP5KI overexpression have not been defined in most cases.

In this study, we report that adenovirus-mediated PIP5KI overexpression in CV1 cells, a fibroblast-like cell line derived from African green monkey kidneys, induces the formation of robust stress fibers and inhibits membrane ruffling after PDGF stimulation. We capitalized on these findings to examine the relation between Rho and PIP5KI and to identify the PIP<sub>2</sub>-regulated players that promote stress-fiber formation and curtail membrane ruffling in these cells.

## Materials and Methods

### Adenovirus-mediated Gene Transfer

Recombinant adenovirus vectors expressing  $\beta$ -gal, hemagglutinin (HA)-tagged mouse PIP5KI $\alpha$  or HA-tagged PIP5KI $\alpha$  (K138A) were constructed as described in Shibasaki et al. (1997). CV1 cells were infected with virus at a multiplicity of 10 for 2 h, washed, and then cultured in serum-free medium for 24 h.

### Fluorescence Microscopy

Cells were fixed in formaldehyde, permeabilized with Triton X-100, and stained with 0.7  $\mu$ M rhodamine-phalloidin for 30 min. Serum-starved cells with thick, longitudinal stress fibers in randomly chosen fields were scored and expressed as a percentage of PIP5KI-overexpressing cells.

Serum-starved CV1 cells (CCL 70; American Type Culture Collection) were stimulated with PDGF (50 ng/ml) for 25 min, and then stained with rhodamine-phalloidin. Cells with dorsal or lateral ruffles (Sun et al., 1997) were counted and expressed as a percentage of PIP5KI-overexpressing cells.

### Inhibitors

Y-27632 compound, a specific inhibitor of Rho-dependent serine/threonine kinase (ROCK; Ishizaki et al., 2000), was provided by M. Uehata (Yoshitomi Pharmaceutical Industries, Osaka, Japan). 2,3-Butanedione 2 monoxide (BDM), a myosin ATPase inhibitor (Cramer and Mitchison, 1995), was obtained from Sigma-Aldrich. HA-1077, a ROCK inhibitor (Weernink et al., 2000), was from Calbiochem.

### Detection of <sup>32</sup>P-labeled Phospholipids in Cells

Cells were labeled for 4 h in phosphate-free DMEM and 40  $\mu$ Ci/ml <sup>32</sup>P-PO<sub>4</sub>. Lipids were extracted, resolved by thin layer chromatography (TLC), and detected by autoradiography (Rozelle et al., 2000). Lipid standards were detected with iodine vapor.

### Phospholipid Mass Quantitation by High Pressure Liquid Chromatography

Cells in a 100-mm dish were washed with ice-cold PBS, rapidly scraped on ice, and fixed with 660  $\mu$ l cold MeOH:HCl (40:1). 330  $\mu$ l CHCl<sub>3</sub> was added, and the sample was transferred to an eppendorf tube (the final solution contains CHCl<sub>3</sub>:MeOH:HCl in a 20:40:1 ratio). The mixture was vortexed vigorously, and 300  $\mu$ l of cold CHCl<sub>3</sub> was added. After centrifugation, the lower phase (containing lipids) was washed with 1 ml MeOH:0.1 M EDTA (1:0.9 vol/vol), and dried under nitrogen. Phospholipids were deacylated by incubation with 1 ml methylamine reagent (25% methylamine in water, MeOH, *n*-butanol; 42.8%:45.8%:11.4%) at 53°C for 50 min (Clarke and Dawson, 1981; Bocckino et al., 1989). The lower phase was dried in a Speed-Vac, resuspended in 0.5 ml water, and extracted twice with an equal volume of *n*-butanol:light petroleum ether:ethyl formate (20:4:1). The aqueous phase was dried under nitrogen, resuspended in water, and subjected to anion-exchange HPLC in an Ionpac AS11 column. Negatively charged glycerol head groups were eluted with a 10–80 mM NaOH gradient and detected online by suppressed conductivity (Talamond et al., 2000) in a Dionex AS50 system equipped with an ASRS-ultra self-regenerating suppressor. Individual peaks were identified with glycerophosphate standards. Peak assignment was validated by spiking some cell samples with purified phospholipids to look for enhance-

ment of specific peaks. The area under each peak was expressed as a function of that of phosphatidylinositol (PI) in the same sample.

### In Vitro Kinase Assay

Phosphoinositide kinase activity was determined as described previously (Chong et al., 1994; Weernink et al., 2000). Cells in 24-well plates were lysed in 100  $\mu$ l of lysis buffer containing (mM): 25 Tris-HCl, pH 7.4, 5 MgCl<sub>2</sub>, 1 EDTA, 0.1 EGTA, and 1 dithiothreitol (kinase buffer) supplemented with 150 NaCl, 10% glycerol, 1% NP-40, 1 sodium orthovanadate, 1 phenylmethylsulfonyl fluoride, 10  $\mu$ g/ml leupeptin, and 0.2 ATP. 10  $\mu$ l lysate was diluted 1:10 with kinase buffer and incubated with 10  $\mu$ M GTP $\gamma$ S and inhibitors at 25°C for 15 min. Kinase reaction was started by the addition of 1  $\mu$ Ci [ $\gamma$ -<sup>32</sup>P]ATP (20  $\mu$ M ATP final concentration), and lipid vesicles containing 70  $\mu$ M PI4P and 35  $\mu$ M phosphatidylserine (PS). Under these conditions, there was a linear increase in <sup>32</sup>P incorporation with time. The reaction was terminated after 10 min at room temperature by adding 1 ml chloroform:methanol:1 N HCl (5:10:4 vol/vol). Lipids extracted in the chloroform phase were spotted on TLC plates.

### Microinjection

Botulinum C3 exoenzyme (C3) ADP-ribosylates and inactivates Rho. Recombinant C3 was obtained by bacterial expression using a glutathione-S-transferase-tagged cDNA clone. The C3 protein was purified by Ni-sepharose chromatography and resuspended in 50 mM Tris-HCl, pH 7.5, 150 mM NaCl, 5 mM MgCl<sub>2</sub>, and 0.1 mM dithiothreitol. Protein concentration was determined using the MicroBCA Protein Assay Kit (Pierce). Cells were microinjected with C3 at a needle concentration of 100 ng/ml together with fluorescein-IgG (3 mg/ml) to serve as an injection marker. After 1 h, cells were fixed, permeabilized, and stained with rhodamine-phalloidin. In some cases, fluorescein-IgG was injected without C3 as a control.

### In Vitro Actin Nucleation Assay

Nucleated actin assembly was quantitated by monitoring the rate of addition of exogenous pyrene-labeled actin in cell lysates (Chan et al., 1998). CV1 cells were stimulated with PDGF (50 ng/ml) for 25 min, and permeabilized with 1% Triton X-100 in a solution containing 60 mM Pipes, 25 mM Hepes, 10 mM EGTA, 2 mM MgCl<sub>2</sub>, 1  $\mu$ M phalloidin, and protease inhibitors, pH 7.4. Pyrene-labeled actin was added to a final concentration of 1  $\mu$ M, and actin polymerization was monitored in a fluorimeter. 2  $\mu$ M cytochalasin B was added to parallel samples to block actin polymerization from the barbed end. Under these conditions, pyrene actin added to buffer alone did not polymerize, and cytochalasin B blocked polymerization from cell lysates by >95%. The rate of barbed-end nucleated actin assembly was obtained by calculating the difference between polymerization in the absence and presence of cytochalasin B. It provides an estimate of the number of polymerization-competent filament barbed ends at the time of cell lysis.

### Protein Pull-down Assays

Gelsolin association with actin monomers was detected using two independent assays. (a) Immunoprecipitation. Cells were lysed in Triton X-100 in the presence of 1 mM EGTA. Gelsolin was immunoprecipitated with 2C4 monoclonal antigelsolin and washed under stringent conditions to depolymerize actin. As a result, all the actin bound to gelsolin are in 1:1 complexes (Chaponnier et al., 1987). The immunoprecipitates were subjected to SDS-PAGE and proteins were detected by Western blotting. In some experiments, cells were metabolically labeled with [<sup>35</sup>S]-translabel (0.2  $\mu$ Ci/ml) for 16 h in methionine-free medium. Immunoprecipitated radioactive bands were detected by autoradiography and their intensity was determined by densitometry scanning. (b) DNaseI-sepharose pull down. Actin monomers bind DNaseI and many proteins that bind actin monomers are pulled down as well. Blank sepharose beads were used as controls for nonspecific binding.

Profilin binding to actin was detected using DNaseI sepharose and poly-L-proline sepharose (Lindberg et al., 1988). Profilin and actin were detected by silver staining or by Western blotting. The polyclonal antiprofilin was generated in our laboratory (Sun et al., 1999), and antiactin was from Sigma-Aldrich.

### Actin Depolymerizing Factor Phosphorylation

An antibody agai-recombinant chicken actin depolymerizing factor (ADF) was generated and affinity purified in our laboratory. The ADF

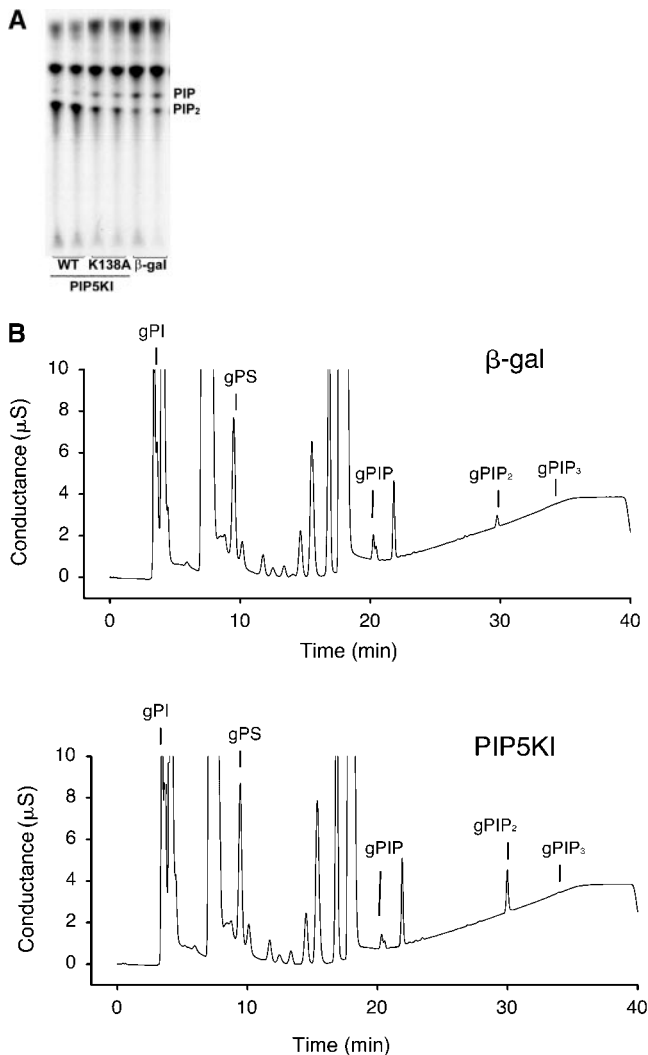


**Figure 1.** Effects of PIP5KI overexpression on PIP<sub>2</sub> levels. CV1 cells were infected with recombinant  $\beta$ -gal, HA-tagged PIP5KI (WT, wild type) or HA-tagged PIP5KI K138A mutant adenovirus vectors, and cultured in serum-free medium. (A) <sup>32</sup>P incorporation into phospholipids. Cells were labeled with <sup>32</sup>P for 4 h. Lipids were extracted, resolved by TLC, and detected by autoradiography. Duplicate samples for each condition were shown. Lipids were identified by using lipid standards. (B) Lipid profiles resolved by HPLC. The elution of glycerol (g)-phospholipid standards was indicated. PS, phosphatidylserine; PI, phosphatidylinositol. Data shown are from a representative experiment repeated three times.

cDNA was a gift of J. Bamberg (Colorado State University, Fort Collins, CO). <sup>32</sup>P-Labeled cells were lysed in 150 mM NaCl, 50 mM Tris HCl, pH 7.2, 2 mM EDTA, 2 mM EGTA, 1% Triton X-100, 0.5% deoxycholate, 0.1% SDS, 50 mM sodium fluoride, 1 mM sodium orthovanadate, 45 mM sodium pyrophosphate, and protease inhibitors (one CompleteMini EDTA-free protease inhibitor tablet/10 ml; Roche). The lysates were centrifuged and used for immunoprecipitation. Immunoprecipitated bands were identified by Western blotting and by autoradiography.

### Fractionation of Actin Pools

Actin pools were assayed by differential centrifugation of Triton X-100 cell extracts (Watts et al., 1991). Lysates were centrifuged sequentially at 15,900 g for 2 min, and then at 366,000 g for 20 min. The pellets from each centrifugation step were resuspended into the original lysate volume. Samples were boiled in SDS gel sample buffer, and equal fractions of each pool were analyzed by SDS-PAGE. Antibodies to capping protein and ezrin were pro-

**Table I.** Effect of PIP5KI Overexpression on Phospholipid Profile

	Cardiolipin/PI	PS/PI	PI4P/PI	PIP <sub>2</sub> /PI
$\beta$ -Gal	1.31 $\pm$ 0.25	0.54 $\pm$ 0.11	0.08 $\pm$ 0.01	0.03 $\pm$ 0.00
PIP5KI	1.20 $\pm$ 0.12	0.56 $\pm$ 0.28	0.03 $\pm$ 0.00	0.06 $\pm$ 0.01

Lipids from cells overexpressing PIP5KI or  $\beta$ -gal adenovirus were extracted and deacylated. The extracts were analyzed by HPLC. The area of the peak for each phospholipid was expressed relative to that of phosphatidylinositol. Values given are mean  $\pm$  SEM of three independent experiments.

vided by D. Schaefer (Washington University, St. Louis, MO), S. Tsukita (Kyoto University) and A. Bretscher (Cornell University, Ithaca, NY).

## Results and Discussion

### PIP5KI Overexpression Increases PIP<sub>2</sub> Levels

We used adenovirus to introduce HA-PIP5KI into cells. Immunofluorescence staining with anti-HA showed that close to 95% of the CV1 cells were infected by this procedure. The high percentage of infected cells allowed us to use biochemical assays to determine precisely how the phosphoinositide levels are changed and how individual players in the regulatory pathway are affected. Using TLC to monitor the phosphoinositide levels, we found that in PIP5KI-overexpressing cells, <sup>32</sup>P incorporation into PIP<sub>2</sub> and PI4P in the experiment shown in Fig. 1 A was 380 and 30%, respectively, of that of  $\beta$ -gal-infected cells. These results established the extent to which PIP<sub>2</sub> level was increased, and showed that there was a reciprocal relation between PIP<sub>2</sub> and PI4P. Although PI4P is generally assumed to be present in large excess compared with PIP<sub>2</sub>, our results suggest that the possibility that a subset of the PI4P pools may be limiting in these cells and that PIP5KI overexpression depletes this PI4P pool by converting it to PIP<sub>2</sub>.

We also tested the effect of the PIP5KI K138A mutant that has minimal kinase activity in vitro, but paradoxically was reported to alter the actin cytoskeleton after overexpression (Ishihara et al., 1998). We now find that PIP5KI K138A increased <sup>32</sup>P-PIP<sub>2</sub> level to 210% of control, and decreased PIP synthesis to 41% of control (Fig. 1 A). Although the increase in PIP<sub>2</sub> synthesis is less than that observed with wild-type PIP5KI, it appears to be sufficient to cause a moderate induction of stress fibers (Fig. 2 A). Recently, a bona fide kinase-dead mutant that does not increase PIP<sub>2</sub> stress level in cells has been described (Tolias et al., 2000). This kinase-dead mutant had no effect on the actin cytoskeleton when overexpressed (data not shown).

To determine whether the change in <sup>32</sup>P incorporation reflects a change in the amount of the phosphoinositides, we used a novel nonradioactive detection method to quantitate deacylated lipids (Fig. 1 B). This technique can resolve glycerol-inositol phosphates that are phosphorylated at the 3, 4, or 5 positions (Hilgemann et al., manuscript in preparation). The elution profile showed that PI and PS were not changed after PIP5KI overexpression, but the PIP<sub>2</sub> peak was increased and the PI4P peak was reduced. When these phosphoinositides were expressed as a function of PI, PIP5KI-overexpressing cells had 200 and 37.5% of the PIP<sub>2</sub> and PI4P, respectively, of control cells (Table I). The cardiolipin/PI and PS/PI ratios were not affected significantly. Therefore, the HPLC and TLC determinations were in

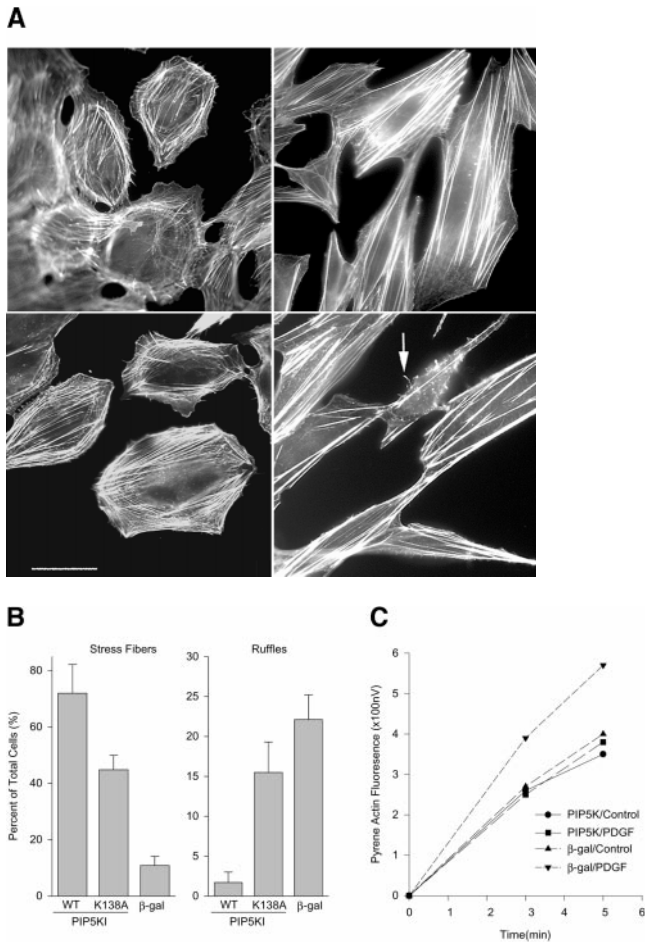


**Figure 2.** Effects of PIP5KI overexpression on the actin cytoskeleton. CV1 cells infected with recombinant HA-PIP5KI, HA-PIP5KI K138A mutant, or  $\beta$ -gal adenovirus were fixed, permeabilized, and stained with rhodamine-phalloidin. (A) Phalloidin staining of actin filaments. (Top left)  $\beta$ -Gal cells. (Right) PIP5KI-overexpressing cells. (Arrow) Actin comets found in a small percentage of cells. (Bottom left) PIP5KI K138A-overexpressing cells. Scale bar, 40  $\mu$ m. (B) Quantitation of cells with robust stress fibers (in the absence of serum) or membrane ruffles (after PDGF treatment). Cells with thick, longitudinal stress fibers or with ruffles in randomly chosen fields were scored and expressed as a percentage of control cells. Data shown is mean  $\pm$  SEM of three experiments. Approximately 100 cells were counted in each category per experiment. (C) In vitro actin nucleation assay. Serum-starved cells stimulated with PDGF or buffer were lysed in Triton X-100. Pyrene-actin monomers were added and the rates of actin polymerization from the ends of filament barbed ends were shown. Data was from a representative experiment, which was repeated three times.

complete agreement, establishing that there was an increase in PIP<sub>2</sub> level and a concomitant decrease in PI4P.

Although PIP<sub>2</sub> is a substrate for the PI 3-kinase, we did not detect an increase in PI(3,4,5)P<sub>3</sub> synthesis after PIP5KI overexpression, using either the TLC (Fig. 1 A) or HPLC (B) methods. Therefore, the PIP5KI-induced actin phenotype is unlikely to be mediated through PI(3,4,5)P<sub>3</sub>.

### PIP5KI Overexpression Induces Stress-Fiber Formation

The PIP5KI-overexpressing CV1 cells cultured in serum-free medium had a markedly different shape and actin cy-

toskeleton than control cells. They were rectangular (Fig. 2 A, top right) and had long, thick stress fibers that were aligned along the cell's longitudinal axis. Their plasma membrane was lined with bright phalloidin staining, suggesting that there is a robust membrane actin cytoskeleton. This is consistent with a recent study showing that PIP<sub>2</sub> maintains the strength of cytoskeletal-plasma membrane adhesion (Raucher et al., 2000). In contrast, control cells were polygonal and had wispy actin filaments characteristic of serum-starved cells (Fig. 2 A, top left). Their actin filament bundles were much shorter and not aligned longitudinally. Their plasma membrane was only weakly stained with phalloidin.

On rare occasions (<3% of cells), actin comet tails were found in PIP5KI-overexpressing CV1 cells, and some of these comets protrude from the plasma membrane (Fig. 2 A, bottom right, arrow). As described previously, cells forming comets have decreased stress fibers (Rozelle et al., 2000). Addition of serum or PDGF did not increase the rate of comet formation in CV1 cells (data not shown). In contrast, PIP5KI-overexpressing REF52 cells and Swiss 3T3 cells generate comets predominantly and dissolve stress fibers (Rozelle et al., 2000). We cannot explain why PIP5KI generates such different phenotypes in the three cell lines examined thus far, but we suspect that the dominance of a unique subset of regulatory proteins within each cellular context determines the final outcome.

PIP5KI K138A also increased stress fibers in CV1 cells, but to a lesser extent than the wild-type enzyme (Fig. 2 A, bottom left). The cells were not as elongated. The milder phenotype is consistent with reduced PIP<sub>2</sub> synthesis (Fig. 1).

Direct quantitation shows that while only  $10.8 \pm 3.3\%$  of  $\beta$ -gal adenovirus-infected cells had thick stress fibers,  $72.0 \pm 10.2\%$  and  $44.8 \pm 5.2\%$  of the PIP5KI wild-type and K138A-overexpressing cells had thick stress fibers, respectively (Fig. 2 B).

### PIP5KI Overexpression Inhibits Membrane Ruffling

Growth factors induce membrane ruffling by promoting actin polymerization from the barbed ends of actin nucleating sites under the plasma membrane (Chan et al., 1998; Svitkina and Borisy, 1999; Borisy and Svitkina, 2000; Cooper and Schafer, 2000). We examined the effect of PIP5KI on PDGF-induced membrane ruffling. Direct counting shows that while  $22.1 \pm 3.1\%$  of control cells formed ruffles after PDGF treatment, only  $1.7 \pm 1.3\%$  of PIP5KI-overexpressing cells did so (Fig. 2 B).

Because ruffling requires the coordinated activation of many actin regulatory proteins, the inability to ruffle could be due to a variety of problems. These include the inability to generate polymerization-competent actin nucleation sites, limited availability of actin monomers for polymerization, and slower rate of actin addition to the barbed ends of the actin nuclei. To sort out some of these possibilities, we used an in vitro actin nucleation assay to determine whether PIP5KI-overexpressing cells were able to generate actin nucleation sites in response to PDGF. As described previously (Azuma et al., 1998; Chan et al., 1998), the lysates of PDGF-treated control cells had a higher rate of barbed end actin assembly (Fig. 2 C). In contrast, cell extracts from PDGF-treated PIP5KI-overexpressing cells did not show an increase in actin nucleation.

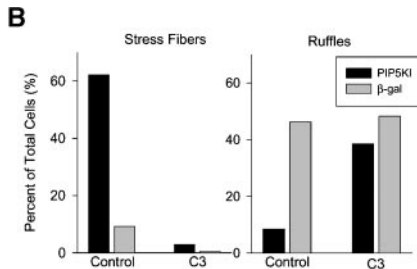
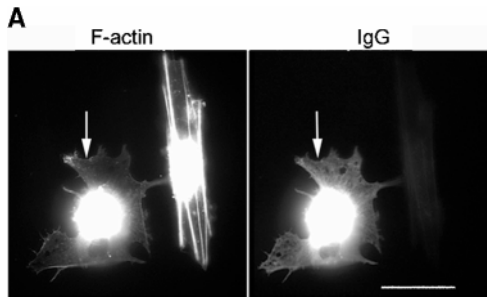


**Figure 3.** PIP5KI-induced stress-fiber formation is blocked by C3. CV1 cells were microinjected with purified C3 and fluorescein-IgG as an injection marker. After 30 min, cells were fixed, permeabilized, and stained with rhodamine-phalloidin. (A) Pair-wise images of rhodamine-phalloidin and fluorescein-IgG staining of two PIP5KI-overexpressing cells. The cell on the left was microinjected with C3 and fluorescein-IgG (arrow), and the one on the right was not injected. Scale bar, 40  $\mu$ m. (B) Quantitation of the effect of C3 on stress-fiber formation and PDGF-induced membrane ruffling. Cells were microinjected with either C3 or fluorescein-IgG or with fluorescein-IgG alone (control). 60–80 microinjected cells were counted in each category, and the percentage of cells with thick stress fibers (in serum-starved conditions) or ruffles (after PDGF treatment) was indicated on the y axis. Data shown is from a single microinjection experiment, which is representative of two experiments.

Thus, inhibition of membrane ruffling could be due to an inability to generate actin nuclei. Polymerization-competent actin nucleating sites are formed by a number of mechanisms (Yin and Stull, 1999). These include severing actin filaments by gelsolin and ADF/cofilin, uncapping of preexisting nuclei by dissociation of capping protein (also

known as CapZ), or de novo formation of actin nuclei through the WASP:Arp2/3 complex pathway. We will describe experiments to identify the basis for the inability to mount an actin polymerization response.

### The Relation between PIP5KI, Rho, and ROCK

We used inhibitors to examine how Rho may be involved in the PIP5KI-induced actin phenotype. Microinjected C3 decreased stress-fiber formation in PIP5KI-overexpressing cells significantly, establishing that Rho is involved. C3 also restored membrane ruffling (Fig. 3, A and B). Since C3 did not stimulate ruffling of  $\beta$ -gal cells, we conclude that membrane ruffling was inhibited as a result of excess stress-fiber formation.

Rho activates multiple effectors that can promote stress-fiber formation (Maekawa et al., 1999; Watanabe et al., 1999) (see Fig. 9). Among these, ROCK has recently been implicated in the stimulation of PIP<sub>2</sub> synthesis (Weernink et al., 2000), inhibition of ADF/cofilin through LIM kinases (Arber et al., 1998; Yang et al., 1998; Sumi et al., 1999), and activation of actomyosin by inhibiting the myosin light chain phosphatase (Kimura et al., 1996). We therefore tested the effect of a specific, cell-permeant ROCK inhibitor, Y-27632, on PIP5KI-induced stress-fiber formation and PIP<sub>2</sub> synthesis. Y-27632 dramatically reduced stress fibers in PIP5KI-overexpressing cells and reduced their plasma membrane phalloidin staining (Fig. 4).

The most straightforward explanation for the inability of PIP5KI overexpression to overcome Y-27632 inhibition was that PIP5KI acts upstream of ROCK. However, this may be overly simplistic. It is also possible that PIP5KI acts downstream of ROCK but is regulated by ROCK even when overexpressed. Another possibility is that ROCK and PIP5KI are not directly linked, and that Y-27632 inhibited the players required for stress-fiber formation without changing PIP<sub>2</sub> concentrations. To distinguish between these possibilities, we examined the effect of Y-27632 on PIP<sub>2</sub> levels. Using TLC, we found that Y-27632 reduced <sup>32</sup>P incorporation into PIP<sub>2</sub> by intact cells significantly (to 64.4  $\pm$  13.3%) (Fig. 5 A; Table II). At the same time, PI4P labeling was also decreased (to 49.8  $\pm$  7.0%). HPLC measurements using unlabeled cells confirmed that there was a decrease in PIP<sub>2</sub>/PI and PI4P/PI mass ratios

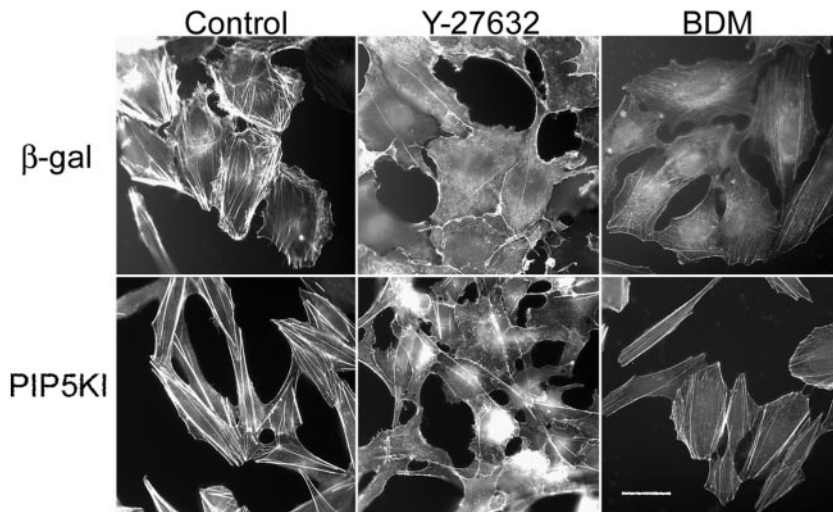


**Figure 4.** Effect of ROCK and myosin ATPase inhibitors on the actin cytoskeleton. Cells were incubated with cell-permeant inhibitors and stained with rhodamine-phalloidin. (Top)  $\beta$ -Gal adenovirus-infected cells after incubation with 1  $\mu$ M Y-27632 or 10 mM BDM for 1 h. (Bottom) PIP5KI overexpressing cells. Scale bar, 40  $\mu$ m.

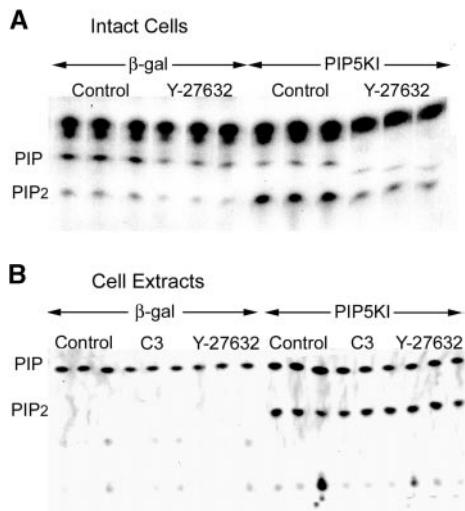


**Figure 5.** Effect of Y-27632 on phosphoinositide synthesis. Incorporation of  $^{32}\text{P}$  into phospholipids was determined by autoradiography after TLC. (A) Intact cells. Cells were radiolabeled with  $^{32}\text{P}$  for 4 h and treated with  $1\ \mu\text{M}$  Y-27632 at the last hour of the labeling period. Result shown is from a single representative experiment done in triplicate. There was a slight retardation of the PI4P band in the Y-27632-treated PIP5KI-overexpressing cells, due to problems with solvent development during the TLC analysis. (B) In vitro kinase assays. Lysates were prepared from cells treated with Y-27632 as described in A, or from untreated cells.  $10\ \mu\text{M}$  Y-27632 was added to the former lysates, and  $10\ \mu\text{g/ml}$  C3 or buffer was added to the latter lysates. The samples were incubated for 15 min at room temperature before the initiation of the kinase assay. PIP<sub>2</sub> synthesis by  $\beta$ -gal cells was too low to be detected at this exposure. Results from multiple experiments were summarized in Table II.

(Table II). The decrease is specific for these lipids because cardiolipin/PI and PS/PI ratios in PIP5KI-overexpressing cells were not changed significantly from that of control cells ( $99.4 \pm 7.9\%$  and  $101.0 \pm 10.8$ , respectively,  $n = 4$ ).

The parallel decrease in PI4P and PIP<sub>2</sub> synthesis in intact cells raises the possibility that Y-27632 reduces PIP<sub>2</sub> synthesis by inhibiting PI4P synthesis, rather than by directly inhibiting PIP5KI. We therefore examined the effect of Y-27632 on phosphoinositide synthesis in cell lysates, under conditions in which PI4P was not limiting. Lysates from PIP5KI-overexpressing cells actively synthesized both PIP<sub>2</sub> and PIP, while those from control cells synthesize much less PIP<sub>2</sub> (Fig. 5 B).

Y-27632 inhibited PI4P synthesis slightly in both lysates, but had no effect on PIP<sub>2</sub> synthesis (Fig. 5 B; Table II). The lack of effect on PIP<sub>2</sub> synthesis in vitro contrasts strikingly with the repression of PIP<sub>2</sub> synthesis by Y-27632 in living cells (Fig. 5 A). Likewise, HA-1077 (another ROCK inhibitor) (Weernink et al., 2000) and C3 also inhibited PI4P but not PIP<sub>2</sub> synthesis (Fig. 5 B; Table II).

The lack of effect of the ROCK inhibitors on PIP<sub>2</sub> synthesis in cell lysates can be explained in several ways. One possibility is that detergent extraction disrupts the cytoskeleton that mediates ROCK regulation of PIP5KI. Another is that Y-27632 does not inhibit PIP5KI directly, but affects PIP<sub>2</sub> synthesis indirectly by limiting the availability of PI4P to PIP5KI in cells. This possibility is supported by

**Table II.** Effects of Rho Inhibitors on Phosphoinositide Profile

Inhibitor	PI4P		PIP <sub>2</sub>	
		<i>n</i>		<i>n</i>
In vivo				
Y-27632				
TLC	$49.8 \pm 7.0$	6	$64.4 \pm 13.3$	6
HPLC	$58.0 \pm 5.8$	4	$57.4 \pm 10.9$	4
In vitro				
HPLC				
Y-27632	$80.9 \pm 3.4$	8	$107.0 \pm 12.1$	6
HA-1077	$83.3 \pm 6.3$	6	$99.9 \pm 9.1$	3
C3	$84.2 \pm 2.2$	2	ND	

Phosphoinositide synthesis was determined using intact cells (in vivo) and in cell lysates by in vitro kinase assays. Phosphoinositide content was determined by analyzing lipids extracted from  $^{32}\text{P}$  labeled cells, or by HPLC of unlabeled cells. CV1 cells were treated with  $1\ \mu\text{M}$  Y-27632 for 1 h, and prepared for lipid analysis. In vitro kinase assays were performed as described in the text, and the lysates were preincubated with  $10\ \mu\text{M}$  Y-27632,  $10\ \mu\text{M}$  HA-1077, or  $0.1\ \text{mg/ml}$  C3 for 15 min before the start of the kinase reaction. Values from inhibitor-treated cells were expressed as a percentage (mean  $\pm$  SEM) of untreated cells. *n*, number of experiments per group.

the fact that overexpression of PIP5KI depletes PI4P (Fig. 1, A and B). It should be pointed out that, although ROCK stimulates PIP<sub>2</sub> synthesis in cells (Weernink et al., 2000), and PIP5KI binds Rho (albeit in a GTP-independent manner; Ren et al., 1996), there is no evidence in the literature to show conclusively that Rho or ROCK directly activates PIP5KI (Ren et al., 1996; Weernink et al., 2000). The possibility that ROCK may regulate the synthesis of phosphoinositides other than PIP<sub>2</sub> has not been considered previously and should be examined further.

It is known that actomyosin contraction promotes stress-fiber formation (Chrzanowska-Wodnicka and Burridge, 1996) and that ROCK promotes contraction by repressing the myosin light chain phosphatase (Kimura et al., 1996). We compared the effect of Y-27632 with that of BDM, which inhibits the myosin ATPase directly. While Y-27632 or BDM both blocked the stress-fiber formation, the BDM-treated PIP5KI-overexpressing cells retained their rectangular shape and the phalloidin staining of their plasma membrane, while the Y-27632-treated cells did not (Fig. 4). These differences suggest that Y-27632 blocks stress-fiber formation in PIP5KI-overexpressing cells not only by inhibiting myosin, but also by other mechanisms, some of which may be linked to the production of PIP<sub>2</sub>.

### Effects of PIP5KI Overexpression on PIP<sub>2</sub>-regulated Actin-severing Proteins

The formation of robust actin stress fibers and the inability to ruffle described here for PIP5KI-overexpressing cells are strikingly similar to the phenotype of gelsolin null fibroblasts (Witke et al., 1995; Azuma et al., 1998). Gelsolin is the most potent actin filament-severing protein identified to date (Sun et al., 1999). Genetic and biological studies have shown that gelsolin is a Rac effector that mediates dynamic actin turnover during membrane ruffling (Azuma et al., 1998). It is inhibited by PIP<sub>2</sub> in vitro. Inhibition of gelsolin by increasing PIP<sub>2</sub> in vivo is therefore expected to prevent it from severing actin filaments in cells, although this has not been demonstrated experimentally.

We therefore tried to determine whether PIP5KI overexpression inhibits gelsolin to generate a de facto gelsolin null phenotype. The gelsolin immunoprecipitates con-

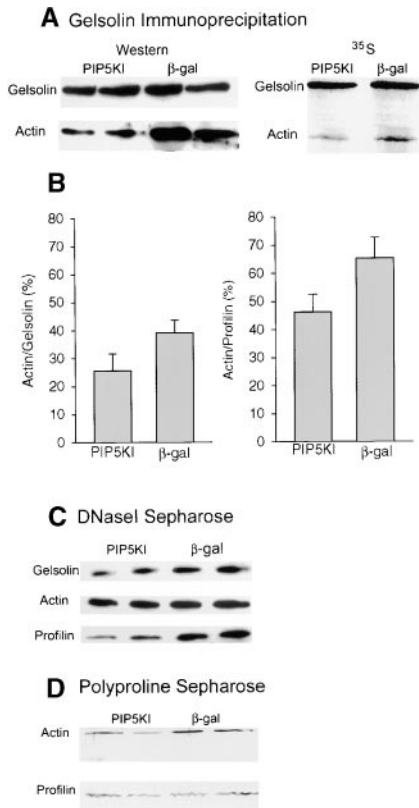


**Figure 6.** Effects of PIP5KI overexpression on the interaction of gelsolin and profilin with actin. (A) Gelsolin immunoprecipitation. Cells were labeled with <sup>35</sup>S-translabel and gelsolin was immunoprecipitated. Gelsolin and actin were detected by Western blotting (left) or by autoradiography (right). (B) Quantitation of actin:gelsolin and actin:profilin ratios after immunoprecipitation. Gelsolin was immunoprecipitated from <sup>35</sup>S-labeled cells as in A, and the intensities of the actin band in the autoradiogram was expressed as a percentage of that of gelsolin. Profilin was pulled down with poly-L-proline sepharose. Profilin and actin was detected by Western blotting, and the intensity of the actin band was expressed as a percentage of that of profilin. Values shown are mean ± SEM of four experiments for gelsolin and two for profilin. (C) Actin pull down with DNaseI-sepharose. Actin and associated gelsolin and profilin were detected by Western blotting. (D) Profilin pull down with poly-L-proline sepharose. Proteins were detected by silver staining.

tained actin (Fig. 6 A), and more actin was coimmunoprecipitated from β-gal than PIP5KI-overexpressing cells. Densitometry scanning showed that the actin:gelsolin <sup>35</sup>S intensity ratio was reduced by 34.8% (from 39.4 ± 4.4% to 25.7 ± 5.9%, *n* = 4, respectively; Fig. 6 B).

Gelsolin interaction with actin was also determined using DNaseI-sepharose to pull down actin monomers, and proteins that bind actin monomers (Fig. 6 C). PIP5KI overexpression reduced the amount of actin associated with gelsolin by 34.6% (actin:gelsolin staining intensity ratio changed from 1.91 to 1.25, *n* = 2). Thus, using two very different methods, we find that gelsolin binding to actin was inhibited to the same extent after PIP5KI overexpression. Since gelsolin stoichiometrically severs actin filaments, this is indicative of a decrease in actin filament severing. This level of inhibition was apparently sufficient to recapitulate the gelsolin-null phenotype obtained by completely elimi-

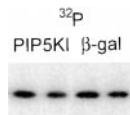


**Figure 7.** PIP5KI overexpression did not affect ADF phosphorylation. ADF was immunoprecipitated from cells labeled with <sup>32</sup>P-PO<sub>4</sub>. Immunoprecipitates were analyzed by autoradiography after SDS PAGE. The first lane in each group was loaded with 1.3× as much sample as the second lane. Western blotting confirmed that the immunoprecipitates from the PIP5KI or control cells had similar amounts of ADF (not shown).

nating the gelsolin gene, probably because other severing proteins, such as ADF/cofilin, was inhibited as well.

ADF/cofilin is a weaker severing protein than gelsolin, but it can profoundly decrease filament length by promoting actin dissociation from the pointed ends of actin filaments (Carrier et al., 1999). ADF/cofilin is inhibited by phosphoinositides (Yonezawa et al., 1990). Unfortunately, we were not able to determine whether PIP5KI overexpression altered ADF interaction with actin, because we could not detect ADF binding to actin, using immunoprecipitation or DNaseI-sepharose. As an alternative approach, we examined the effect of PIP5KI overexpression on the phosphorylation state of ADF. ADF is inhibited by LIM kinase, which is activated by ROCK (Arber et al., 1998; Sumi et al., 1999). Endogenous ADF was immunoprecipitated from <sup>32</sup>P-labeled cells (Fig. 7). In duplicate experiments, the <sup>32</sup>P-ADF/total ADF level of PIP5KI-overexpressing cells was 93.9% of that of β-gal-overexpressing control cells. Thus, PIP5KI overexpression had no effect on ADF phosphorylation. It remains to be shown whether ADF/cofilin interaction with actin is reduced by PIP<sub>2</sub> in PIP5KI-overexpressing cells.

### Effects of PIP5KI Overexpression on Other Actin Regulatory Proteins that Promote Dynamic Actin Assembly

Recently, there is increasing evidence that WASP:Arp2/3 complexes drive de novo actin assembly from membranes to promote membrane ruffling and vesicle trafficking (Rohatgi et al., 2000; Rozelle et al., 2000). WASP and related members such as N-WASP are activated by PIP<sub>2</sub> (Miki et al., 1996; Higgs and Pollard, 2000; Rohatgi et al., 2000). It is therefore puzzling that CV1 cells do not mount a vigorous actin polymerization response to PDGF, as evidenced by the lack of ruffling or comet formation (Fig. 2, A and B), or generation of polymerization competent actin nuclei (C), even though N-WASP should presumably be activated by PIP<sub>2</sub> in these cells, and a substantial actin monomer pool is still available (Fig. 8).

We therefore examined some of the other components that promote nucleated actin assembly from WASP:Arp2/3 complexes (Loisel et al., 1999; Blanchoin et al., 2000; Borisy and Svitkina, 2000). Capping protein works primarily to terminate polymerization (Eddy et al., 1997) and to funnel actin monomers to privileged actin nuclei generated at the WASP:Arp2/3 interface. Profilin, although not absolutely required for comet formation, increases the rate of actin polymerization by acting synergistically with ADF/cofilin (Didry et al., 1998; Loisel et al., 1999) and prevents spontaneous actin polymerization. Both proteins are inhibited by PIP<sub>2</sub> in vitro (Lassing and Lindberg, 1985; Schafer et al., 1996).

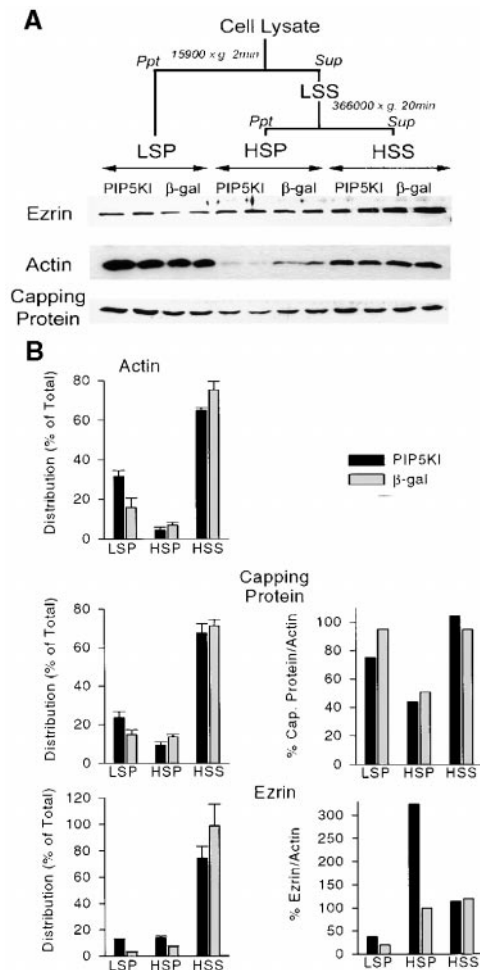


**Figure 8.** Effects of PIP5KI overexpression on the partitioning of proteins into Triton X-100 soluble and insoluble fractions. (A) Fractionation of actin pools by differential centrifugation. (Top) Flow chart, (bottom) protein distribution among the different pools. Equal fractions of each pool were electrophoresed in SDS-polyacrylamide gels and subjected to Western blotting. The blots shown were representative of four independent experiments. (B) Bar graphs depicting the partitioning of actin, capping protein, and ezrin. The protein distribution in each pool was expressed as a percentage of the total (left). Values shown were mean  $\pm$  SEM ( $n = 4$ ). The amount of capping protein and ezrin was also expressed as a percentage of actin in the same fraction (right). Data from a single representative experiment was shown.

Profilin:actin interaction was detected by using polyproline-sepharose to bind profilin and DNAseI-sepharose to bind actin. PIP5KI overexpression induced a 40% decrease in actin associated with profilin bound to polyproline beads (Fig. 6, B and D), and a 51% decrease in profilin bound to actin associated with DNaseI-sepharose (Fig. 6 C).

Capping protein interaction with actin filaments was monitored by differential centrifugation to obtain functionally defined actin compartments (Fig. 8 A). Low speed centrifugation sediments highly cross-linked actin filaments including stress fibers (low-speed pellet, LSP). Actin filaments that are not cross linked into thick bundles can be sedimented into the high-speed pellet (HSP) by further centrifugation of the low-speed supernatant. Actin monomers and short oligomers remain in the high-speed supernatant (HSS).

PIP5KI overexpression increased the amount of actin recovered in the LSP to 201% of control, and decreased that in the HSP by 40%. Nevertheless, the bulk of the cellular actin remained in the HSS, and there was only a 14% difference between PIP5KI and  $\beta$ -gal-overexpressing cells. This is in agreement with the report that Rho does not increase actin polymerization substantially when it induces stress-fiber formation (Machesky and Hall, 1997). Our results suggest that increased stress fiber density and thickness in PIP5KI-overexpressing cells are due primarily to the recruitment of polymerized actin from the HSP to the LSP, and the inability to ruffle is not due to the lack of actin monomers per se.

PIP5KI-overexpressing cells had more capping protein in the LSP (159% of control), and less in the HSP (decrease by 31%) (Fig. 8 B). However, when the capping protein was expressed as a ratio to actin in the same fraction, there was a significant decrease in the LSP, a smaller decrease in the HSP, and an increase in the HSS (Fig. 8 B). These results show that PIP<sub>2</sub> inhibits capping protein in vivo, as suggested previously by in vitro studies (Schafer et al., 1996). Since capping protein binds only to the barbed end of an actin filament, the filaments in the LSP and HSP of PIP5KI-overexpressing cells are likely to be longer than those in control cells. In conclusion, the stress fiber and nonruffling phenotype can be explained by PIP<sub>2</sub> inhibition of actin severing by gelsolin and ADF/cofilin, inhibition of capping protein, and inhibition of profilin.

#### Effect of PIP5KI Overexpression on Ezrin

Proteins in the ezrin/radixin/moesin family (ERM) cross link actin filaments to the plasma membrane (Hirao et al., 1996). They are required for the reconstitution of Rho-dependent stress fiber and focal contact formation in permeabilized cells (Mackay et al., 1997), and they are activated by PIP<sub>2</sub> in vitro (Hirao et al., 1996). PIP5KI overexpression in NIH3T3 cells enhances ERM phosphorylation and induces microvilli formation without increasing stress fibers (Matsui et al., 1999). Since our PIP5KI-overexpressing CV1 cells do not form microvilli but have thick stress fibers, we wanted to know if ezrin is involved.

PIP5KI overexpression increased ezrin association with actin filaments increased in the HSP and LSP and reduced that in the HSS (Fig. 8 B). These differences are particularly striking when ezrin was expressed as a function of actin. The ezrin/actin ratios are doubled and tripled in the LSP and HSP, respectively. A dramatic increase in ezrin binding to actin suggests that ezrin is likely to be the PIP<sub>2</sub> regulator of membrane-cytoskeletal linkage.

#### A Model for How PIP<sub>2</sub> Induces Stress-Fiber Formation

In conclusion, PIP5KI overexpression in CV1 cells stimulates stress-fiber formation, inhibits PDGF-induced membrane ruffling, and blocks the generation of polymerization-competent actin nuclei. The PIP5KI effect is dependent on PIP<sub>2</sub> synthesis; the PIP5KI mutant K138A is less effective in increasing PIP<sub>2</sub> level and is also less effective in promoting stress-fiber formation and blocking membrane ruffling. Stress-fiber formation has been ascribed to Rho activation, and membrane ruffling to Rac activation (Hall, 1998). The reciprocal effects of PIP5KI overexpression on stress-fiber formation and membrane ruffling suggest that the Rho dominates within the context of the CV1 cells, and this suppresses Rac-dependent actin



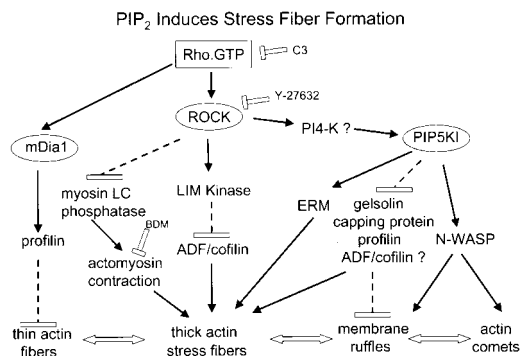


**Figure 9.** Proposed involvement of PIP<sub>2</sub> in stress-fiber assembly. The model is adapted from Maekawa et al. (1999) and Watanabe et al. (1999), and incorporates the finding that generation of a particular actin structure reflects the antagonistic as well as cooperative influences of multiple inputs. PIP5KI is regulated by multiple mechanisms. In this diagram, we focus on the Rho pathway, and show that the increase in PIP<sub>2</sub> synthesis after PIP5KI overexpression is at least partly mediated through ROCK, because the ROCK inhibitor Y-27632 decreases PIP<sub>2</sub> accumulation in cells. Our data suggest that inhibition may be due to a decrease in PI4P synthesis, although this is not yet established conclusively (?). The inhibitors used, and their sites of action, are indicated. The effect of PIP5KI overexpression on ADF/cofilin function was not determined, and hence the potential involvement of ADF/cofilin is denoted by a question mark. (Two-headed arrows) Reciprocal antagonistic actions, (black arrow) activation. The bar at the end of dashed line indicates inhibition after PIP5KI overexpression in CV1 cells. The dominance of signals to generate stress fibers in CV1 decreases the ability of the cells to ruffle their membrane, to form thin actin fibers, and to form actin comets.

structures. This mutually exclusive cytoskeletal response to Rho and Rac is supported by many other studies (Burrige, 1999; Rottner et al., 1999; Sander et al., 1999; Bito et al., 2000). In our previous study, we found that overexpression of PIP5KI in two other types of cells generates actin comets, decreases stress fibers, and suppresses membrane ruffling (Rozelle et al., 2000) through pathways that may be mediated by Cdc42. Therefore, the reciprocal antagonism between these small GTPases and their downstream effectors may explain why a particular actin phenotype dominates after PIP5KI overexpression, and that the phenotype is dependent on the cellular context.

PIP5KI induction of stress fibers can be considered in this context (Fig. 9). Watanabe et al. (1999) proposes that Rho promotes actin reorganization by a cooperative model. In this scheme, thick stress-fiber assembly is activated by ROCK kinase and antagonized by the mDia1 pathway, which uses profilin to form thin actin fibers. We show that PIP5KI overexpression altered the activity of several key actin regulatory proteins. We propose that these changes may account for the increase in thick stress fibers and inhibition of the mDia1 and Rac pathways. First, gelsolin is inhibited from severing actin filaments. This increases the overall length distribution of actin filaments and promotes bundling into stress fibers. It also decreases the number of actin nuclei that can be used to mount an actin nucleation response downstream of Rac activation. The PIP5KI overexpression phenotype is remarkably similar to that of gelsolin-null cells, supporting a cause and effect relation. Although we did not show that ADF/cofilin is inhibited as well (Fig. 9, ?), this is likely to be the case. Second, capping protein is inhibited, so actin

polymerization is not terminated in a timely manner. As a result, filaments are longer and more readily cross linked into stress fibers. Third, profilin binding to actin is also reduced. The decrease in monomer sequestering capacity may promote spontaneous actin polymerization to account for the small increase in polymerized actin observed in Fig. 8. Inhibition of profilin will decrease the rate of filament elongation (Didry et al., 1998). Profilin inhibition will also compromise the mDia1 pathway (Watanabe et al., 1999). The balance is therefore shifted towards the formation of thick stress fiber in the antagonist ROCK stress-fiber pathway. Fourth, PIP<sub>2</sub> promotes the activation of ERM to stabilize membrane-cytoskeletal linkage. ERM may in turn activate Rho in a positive feedback loop (Matsui et al., 1999). The upregulation of integrin signaling can further activate Rho through bidirectional signaling (Schoenwaelder and Burrige, 1999).

PIP5KI overexpression inhibited membrane ruffling in all three types of cells examined thus far (this study; Rozelle et al., 2000). Inhibition of ruffling is likely to be due to PIP<sub>2</sub> inhibition of gelsolin, capping protein, and profilin. These proteins generate actin nucleation sites, promote “funneling” of actin monomers to privileged sites, and ensure the continued supply of actin monomers to fuel actin polymerization. Some (capping protein) are essential components of the N-WASP:Arp2/3 actin polymerization machinery (Loisel et al., 1999), explaining why membrane ruffling is inhibited even when N-WASP itself should be activated by PIP<sub>2</sub>. The others (e.g., gelsolin and profilin) clearly have been implicated in dynamic actin reorganization. Our *in vitro* nucleation assay shows that there is a decrease in the number of polymerization-competent actin nuclei, which would be consistent with inhibition of actin nucleation *per se*. It is therefore reasonable to conclude that besides N-WASP, which is activated by PIP<sub>2</sub>, another target that is inhibited by PIP<sub>2</sub> may also have a role in generating actin nucleation sites.

Although Rac and Rho have each been implicated in the activation of PIP5KI and LIM kinases, the balance in CV1 cells is tipped in favor of the Rho pathway. A similar antagonism has also been observed between membrane ruffling and actin comet formation, even though both use PIP<sub>2</sub> and N-WASP (Rozelle et al., 2000). We therefore propose that the reciprocal antagonism between the signals to generate distinct actin structures may explain why increasing PIP<sub>2</sub> in cells can produce pleiotropic actin phenotypes. The data presented here elucidated the pathway by which PIP<sub>2</sub> increases stress-fiber formation and inhibits membrane ruffling, and the involvement of ROCK in these responses.

We thank many colleagues for generously supplying us with reagents used in this study. They are acknowledged individually in the text. We thank A. Rozelle for doing the ADF/cofilin immunoprecipitation experiments.

This work is supported by grants from the National Institutes of Health to H.L. Yin (GM51112 and GM61203) and D.H. Hilgemann (HL51323), and the Welch Foundation to H.L. Yin.

Submitted: 28 November 2000

Revised: 11 January 2001

Accepted: 11 January 2001

#### References

- Arber, S., F.A. Barbayannis, H. Hanser, C. Schneider, C.A. Stanyon, O. Bernard, and P. Caroni. 1998. Regulation of actin dynamics through phosphorylation of cofilin by LIM-kinase. *Nature*. 393:805–809.
- Azuma, T., W. Witke, T.P. Stossel, J.H. Hartwig, and D.J. Kwiatkowski. 1998.

- Gelsolin is a downstream effector of rac for fibroblast motility. *EMBO (Eur. Mol. Biol. Organ.) J.* 17:1362–1370.
- Bito, H., T. Furuyashiki, H. Ishihara, Y. Shibasaki, K. Ohashi, K. Mizuno, M. Maekawa, T. Ishizaki, and S. Narumiya. 2000. A critical role for a Rho-associated kinase, p160ROCK, in determining axon outgrowth in mammalian CNS neurons. *Neuron*. 26:431–441.
- Blanchoin, L., K.J. Amann, H.N. Higgs, J.B. Marchand, D.A. Kaiser, and T.D. Pollard. 2000. Direct observation of dendritic actin filament networks nucleated by Arp2/3 complex and WASP/Scar proteins. *Nature*. 404:1007–1011.
- Bocckino, S.B., P. Wilson, and J.H. Exton. 1989. An enzymatic assay for picomole levels of phosphatidate. *Anal. Biochem.* 180:24–27.
- Borisy, G.G., and T.M. Svitkina. 2000. Actin machinery: pushing the envelope. *Curr. Opin. Cell Biol.* 12:104–112.
- Burridge, K. 1999. Crosstalk between Rac and Rho. *Science*. 283:2028–2029.
- Carlier, M.-F., F. Ressaad, and D. Pantaloni. 1999. Control of actin dynamics in cell motility: role of ADF/cofilin. *J. Biol. Chem.* 274:33827–33830.
- Chan, A.Y., S. Raft, M. Bailly, J.B. Wyckoff, J.E. Segall, and J.S. Condeelis. 1998. EGF stimulates an increase in actin nucleation and filament number at the leading edge of the lamellipod in mammary adenocarcinoma cells. *J. Cell Sci.* 111:199–211.
- Chaponnier, C., H.L. Yin, and T.P. Stossel. 1987. Reversibility of gelsolin/actin interaction in macrophages. Evidence of Ca<sup>2+</sup>-dependent and Ca<sup>2+</sup>-independent pathways. *J. Exp. Med.* 165:97–106.
- Chong, L.D., A. Traynor-Kaplan, G.M. Bokoch, and M.A. Schwartz. 1994. The small GTP-binding protein Rho regulates a phosphatidylinositol 4-phosphate 5-kinase in mammalian cells. *Cell*. 79:507–513.
- Chrzanowska-Wodnicka, M., and K. Burridge. 1996. Rho-stimulated contractility drives the formation of stress fibers and focal adhesions. *J. Cell Biol.* 133:1403–1415.
- Clarke, N.G., and R.M. Dawson. 1981. Alkaline O leads to N-transacylation. A new method for the quantitative deacylation of phospholipids. *Biochem. J.* 195:301–306.
- Cooper, J.A., and D.A. Schafer. 2000. Control of actin assembly and disassembly at filament ends. *Curr. Opin. Cell Biol.* 12:97–103.
- Cramer, L.P., and T.J. Mitchison. 1995. Myosin is involved in postmitotic cell spreading. *J. Cell Biol.* 131:179–189.
- Cremona, O., G. Di Paolo, M.R. Wenk, A. Luthi, W.T. Kim, K. Takei, L. Daniell, Y. Nemoto, S.B. Shears, R.A. Flavell, D.A. McCormick, and P. De Camilli. 1999. Essential role of phosphoinositide metabolism in synaptic vesicle recycling. *Cell*. 99:179–188.
- Didry, D., M.F. Carlier, and D. Pantaloni. 1998. Synergy between ADF/cofilin and profilin in increasing actin filament turnover. *J. Biol. Chem.* 273:25602–25611.
- Eddy, R.J., J. Han, and J.S. Condeelis. 1997. Capping protein terminates but does not initiate chemoattractant-induced actin assembly in *Dictyostelium*. *J. Cell Biol.* 139:1243–1253.
- Hall, A. 1998. Rho GTPases and the actin cytoskeleton. *Science*. 279:509–514.
- Higgs, H.N., and T.D. Pollard. 2000. Activation by Cdc42 and PIP(2) of Wiskott-Aldrich syndrome protein (WASP) stimulates actin nucleation by Arp2/3 complex. *J. Cell Biol.* 150:1311–1320.
- Hirao, M., N. Sato, T. Kondo, S. Yonemura, M. Monden, T. Sasaki, Y. Takai, and S. Tsukita. 1996. Regulation mechanism of ERM (Ezrin/Radixin/Moesin) protein/plasma membrane association: possible involvement of phosphatidylinositol turnover and rho-dependent signaling pathway. *J. Cell Biol.* 135:37–51.
- Honda, A., M. Nogami, T. Yokozeki, M. Yamazaki, H. Nakamura, H. Watanabe, K. Kawamoto, K. Nakayama, A.J. Morris, M.A. Frohman, and Y. Kanaho. 1999. Phosphatidylinositol 4-phosphate 5-kinase is a downstream effector of the small G protein ARF6 in membrane ruffle formation. *Cell*. 99:521–532.
- Ishihara, H., Y. Shibasaki, N. Kizuki, T. Wada, Y. Yazaki, T. Asano, and Y. Oka. 1998. Type I phosphatidylinositol-4-phosphate 5-kinases. Cloning of the third isoform and deletion/substitution analysis of members of this novel lipid kinase family. *J. Biol. Chem.* 273:8741–8748.
- Ishizaki, T., M. Uehata, I. Tamechika, J. Keel, K. Nonomura, M. Maekawa, and S. Narumiya. 2000. Pharmacological properties of Y-27632, a specific inhibitor of rho-associated kinases. *Mol. Pharmacol.* 57:976–983.
- Jones, D.H., J.B. Morris, C.P. Morgan, H. Kondo, R.F. Irvine, and S. Cockcroft. 2000. Type I phosphatidylinositol 4-phosphate 5-kinase directly interacts with ADP-ribosylation factor 1 and is responsible for phosphatidylinositol 4,5-bisphosphate synthesis in the Golgi compartment. *J. Biol. Chem.* 275:13962–13966.
- Kimura, K., M. Ito, M. Amano, K. Chihara, Y. Fukata, M. Nakafuku, B. Yamamori, J. Feng, T. Nakano, K.I.A. Okawa, and K. Kaibuchi. 1996. Regulation of myosin phosphatase by Rho and Rho-associated kinase (Rho-kinase). *Science*. 273:245–248.
- Lassing, I., and U. Lindberg. 1985. Specific interaction between phosphatidylinositol 4,5 bisphosphate and profilactin. *Nature*. 314:472–474.
- Lindberg, U., C.E. Schutt, E. Hellsten, A.C. Tjader, and T. Hult. 1988. The use of poly(L-proline)-sepharose in the isolation of profilin and profilactin complexes. *Biochim. Biophys. Acta*. 967:391–400.
- Loisel, T.P., R. Boujemaa, D. Pantaloni, and M.-F. Carlier. 1999. Reconstitution of actin-based motility of *Listeria* and *Shigella* using pure proteins. *Nature*. 401:613–616.
- Mackay, D.J., F. Esch, H. Furthmayr, and A. Hall. 1997. Rho- and rac-dependent assembly of focal adhesion complexes and actin filaments in permeabilized fibroblasts: an essential role for ezrin/radixin/moesin proteins. *J. Cell Biol.* 138:927–938.
- Machesky, L.M., and A. Hall. 1997. Role of actin polymerization and adhesion to extracellular matrix in Rac- and Rho-induced cytoskeletal reorganization. *J. Cell Biol.* 138:913–926.
- Maekawa, M., T. Ishizaki, S. Boku, N. Watanabe, A. Fujita, A. Iwamoto, T. Obinata, K. Ohashi, K. Mizuno, and S. Narumiya. 1999. Signaling from Rho to the actin cytoskeleton through protein kinases ROCK and LIM-kinase. *Science*. 285:895–898.
- Matsui, T., S. Yonemura, Sh. Tsukita, and Sa. Tsukita. 1999. Activation of ERM proteins in vivo by Rho involves phosphatidylinositol 4-phosphate 5-kinase and not ROCK kinases. *Curr. Biol.* 9:1259–1262.
- Miki, H., K. Miura, and T. Takenawa. 1996. A novel actin-depolymerizing protein, regulates the cortical cytoskeletal rearrangement in a PIP<sub>2</sub>-dependent manner downstream of tyrosine kinases. *EMBO (Eur. Mol. Biol. Organ.) J.* 15:5326–5335.
- Raucher, D., T. Stauffer, W. Chen, K. Shen, S. Guo, J.D. York, M.P. Sheetz, and T. Meyer. 2000. Phosphatidylinositol 4,5-bisphosphate functions as a second messenger that regulates cytoskeleton-plasma membrane adhesion. *Cell*. 100:221–228.
- Ren, X.-D., G.M. Bokoch, A. Traynor-Kaplan, G.H. Jenkins, R.A. Anderson, and M.A. Schwartz. 1996. Physical association of the small GTPase Rho with a 68-kDa phosphatidylinositol 4-phosphate 5-kinase in Swiss 3T3 cells. *Mol. Biol. Cell*. 7:435–442.
- Rohatgi, R., H.Y. Ho, and M.W. Kirschner. 2000. Mechanism of N-WASP activation by CDC42 and phosphatidylinositol 4, 5-bisphosphate. *J. Cell Biol.* 150:1299–1310.
- Rottner, K., A. Hall, and J.V. Small. 1999. Interplay between Rac and Rho in the control of substrate contact dynamics. *Curr. Biol.* 9:640–648.
- Rozelle, A.L., L.M. Machesky, M. Yamamoto, M.H. Driessens, R.H. Insall, M.G. Roth, K. Luby-Phelps, G. Marriott, A. Hall, and H.L. Yin. 2000. Phosphatidylinositol 4,5-bisphosphate induces actin-based movement of raft-enriched vesicles through WASP-Arp2/3. *Curr. Biol.* 10:311–320.
- Sakisaka, T., T. Itoh, K. Miura, and T. Takenawa. 1997. Phosphatidylinositol 4,5-bisphosphate phosphatase regulates the rearrangement of actin filaments. *Mol. Cell Biol.* 17:3841–3849.
- Sander, E.E., J.P. ten Klooster, S. van Delft, R.A. van der Kammen, and J.G. Collard. 1999. Rac downregulates Rho activity: reciprocal balance between both GTPases determines cellular morphology and migratory behavior. *J. Cell Biol.* 147:1009–1022.
- Schafer, D.A., P.B. Jennings, and J.A. Cooper. 1996. Dynamics of capping protein and actin assembly in vitro: uncapping barbed ends by polyphosphoinositides. *J. Cell Biol.* 135:169–179.
- Schoenwaelder, S.M., and K. Burridge. 1999. Bidirectional signaling between the cytoskeleton and integrins. *Curr. Opin. Cell Biol.* 11:274–286.
- Shibasaki, Y., H. Ishihara, N. Kizuki, T. Asano, Y. Oka, and Y. Yazaki. 1997. Massive actin polymerization induced by phosphatidylinositol-4-phosphate 5-kinase in vivo. *J. Biol. Chem.* 272:7578–7581.
- Sumi, T., K. Matsumoto, Y. Takai, and T. Nakamura. 1999. Cofilin phosphorylation and actin cytoskeletal dynamics regulated by rho- and Cdc42-activated LIM-kinase 2. *J. Cell Biol.* 147:1519–1532.
- Sun, H.Q., K.L. Lin, and H.L. Lin. 1997. Gelsolin modulates phospholipase C activity in vivo through phospholipid binding. *J. Cell Biol.* 138:811–820.
- Sun, H.-Q., M. Yamamoto, M. Mejillano, and H.L. Yin. 1999. Gelsolin, a multifunctional actin regulatory protein. *J. Biol. Chem.* 274:33179–33182.
- Svitkina, T.M., and G.G. Borisy. 1999. Arp2/3 complex and actin depolymerizing factor/cofilin in dendritic organization and treadmilling of actin filament array in lamellipodia. *J. Cell Biol.* 145:1009–1026.
- Talamond, P., S. Doulbeau, I. Rochette, and J.P. Guyot. 2000. Anion-exchange high-performance liquid chromatography with conductivity detection for the analysis of phytic acid in food. *J. Chromatogr. A*. 871:7–12.
- Tolias, K.F., J.H. Hartwig, H. Ishihara, Y. Shibasaki, L.C. Cantley, and C.L. Carpenter. 2000. Type I alpha phosphatidylinositol-4-phosphate 5-kinase mediates Rac-dependent actin assembly. *Curr. Biol.* 10:153–156.
- Watanabe, N., T. Kato, A. Fujita, T. Ishizaki, and S. Narumiya. 1999. Cooperation between mDia1 and ROCK in Rho-induced actin reorganization. *Nat. Cell Biol.* 1:136–143.
- Watts, R.G., M.A. Crispens, and T.H. Howard. 1991. A quantitative study of the role of F-actin in producing neutrophil shape. *Cell Motil. Cytoskelet.* 19:159–168.
- Weernink, P.A., Y. Guo, C. Zhang, M. Schmidt, C. Eichel-Streiber, and K.H. Jakobs. 2000. Control of cellular phosphatidylinositol 4,5-bisphosphate levels by adhesion signals and rho GTPases in NIH 3T3 fibroblasts involvement of both phosphatidylinositol-4-phosphate 5-kinase and phospholipase C. *Eur. J. Biochem.* 267:5237–5246.
- Witke, W., A.H. Sharpe, J.H. Hartwig, T. Azuma, T.P. Stossel, and D.J. Kwiatkowski. 1995. Hemostatic, inflammatory, and fibroblast responses are blunted in mice lacking gelsolin. *Cell*. 81:41–51.
- Yang, N., O. Higuchi, K. Ohashi, K. Nagata, A. Wada, K. Kangawa, E. Nishida, and K. Mizuno. 1998. Cofilin phosphorylation by LIM-kinase 1 and its role in Rac-mediated actin reorganization. *Nature*. 393:809–812.
- Yin, H.L., and J.T. Stull. 1999. Proteins that regulate dynamic actin remodeling in response to membrane signaling. *J. Biol. Chem.* 274:32529–32530.
- Yonezawa, N., E. Nishida, K. Iida, I. Yahara, and H. Sakai. 1990. Inhibition of the interactions of cofilin, dectrin, and deoxyribonuclease I with actin by phosphoinositides. *J. Biol. Chem.* 265:8382–8386.